Leukemia (2016) **30**, 1887–1896

www.nature.com/leu

ORIGINAL ARTICLE

CREB engages C/EBPδ to initiate leukemogenesis

C Tregnago[1], E Manara[2], M Zampini[2], V Bisio[1], C Borga[1,3], S Bresolin[1], S Aveic[2], G Germano[2], G Basso[1] and M Pigazzi[1]

cAMP response element binding protein (CREB) is frequently overexpressed in acute myeloid leukemia (AML) and acts as a proto-oncogene; however, it is still debated whether such overactivation alone is able to induce leukemia as its pathogenetic downstream signaling is still unclear. We generated a zebrafish model overexpressing CREB in the myeloid lineage, which showed an aberrant regulation of primitive hematopoiesis, and in 79% of adult CREB-zebrafish a block of myeloid differentiation, triggering to a monocytic leukemia akin the human counterpart. Gene expression analysis of CREB-zebrafish revealed a signature of 20 differentially expressed human homologous CREB targets in common with pediatric AML. Among them, we demonstrated that CREB overexpression increased CCAAT-enhancer-binding protein-δ (C/EBPδ) levels to cause myeloid differentiation arrest, and the silencing of CREB-C/EBPδ axis restored myeloid terminal differentiation. Then, C/EBPδ overexpression was found to identify a subset of pediatric AML affected by a block of myeloid differentiation at monocytic stage who presented a significant higher relapse risk and the enrichment of aggressive signatures. Finally, this study unveils the aberrant activation of CREB-C/EBPδ axis concurring to AML onset by disrupting the myeloid cell differentiation process. We provide a novel *in vivo* model to perform high-throughput drug screening for AML cure improvement.

Leukemia (2016) **30,** 1887–1896; doi:10.1038/leu.2016.98

INTRODUCTION

The cAMP response element binding protein (CREB) is one of the most important transcription factors that play a crucial role in normal and neoplastic hematopoiesis, governing many critical cellular processes, included proliferation and differentiation of myeloid progenitor cells.[1] Further studies demonstrated that enforced expression of CREB promoted growth and survival of healthy bone marrow cells through the upregulation of specific downstream target genes, whereas its downregulation in acute myeloid leukemia (AML) cell lines and primary cultures suppressed cell proliferation and lowered clonogenic tumor ability.[2–4] Transgenic mice overexpressing CREB developed aberrant monocytosis and, after a prolonged latency of 2 years, a myeloproliferative disease with high white blood cell count and abnormal myelopoiesis.[1]

CREB overexpression has been found in patients with AML and acute lymphoblastic leukemia, contributing to decreased event-free survival of patients.[1,5,6] Different mechanisms that lead to CREB overexpression have been dissected, such as *CREB1* gene amplification,[1] lack of CREB endogenous modulator inducible cAMP early repressor (ICER)[3,7] and downregulation of CREB translational regulator miR-34b through an epigenetic mechanism.[8,9] Thus, there are both clinical and experimental data that support CREB as a critical proto-oncogene of myeloid transformation, but till now the pathways and genes directly controlled by CREB that trigger leukemia are unknown.

Considering that 66% of pediatric AML exhibit high levels of CREB,[5] the dissection of its leukemogenic mechanisms could have both biological and clinical relevance. Indeed, despite the use of intensive and multimodality treatment, established through prospective clinical trials by cooperative groups of the pediatric oncology research community, 30% of children and adolescents with AML still die from their disease, and late effects will adversely influence their adult life.[10–13] Tumor heterogeneity represents the most important challenge for the development of molecularly targeted anticancer therapies in pediatric tumors,[14–17] and thus in this field the creation of *in vivo* models to dissect AML biology is highly recommended to develop new treatment opportunities.[18,19]

Over the past decade, zebrafish (*Danio rerio*) has emerged as a useful model to study cancer, in particular leukemia.[20–30] Of note, *creb* gene sequence and functional domains, such as the kinase-inducible domain and the DNA-binding domain, are highly conserved between zebrafish and mammals. Creb function was previously investigated in zebrafish developmental studies, revealing its crucial physiological activity, as Creb mutants resulted in altered brain and neural structure development.[31]

In this work, we present a CREB-zebrafish transgenic model where CREB expression has been driven in the hematopoietic compartment for studying its role in embryonic and adult myelopoiesis. We characterized the induced malignancy by gene expression profile and found that *c/ebpδ* was the key CREB target in triggering cell transformation through the arrest of the myeloid differentiation process at monocytic stage, with a complete loss of precursors. These same zebrafish leukemic features of high CCAAT-enhancer-binding protein-δ (C/EBPδ) levels and monocytic myeloid blasts were found in a subset of pediatric patients affected by *de novo* AML with a severe prognosis. We demonstrated that C/EBPδ overexpression was able to rescue CREB silencing effects on differentiation, confirming its role in AML. Finally, this study identifies a novel CREB-C/EBPδ axis crucial for leukemogenesis, and provides a new attractive zebrafish model for high-throughput screening to improve AML therapeutic strategies.

[1]Women and Child Health Department, Hematology-Oncology Clinic, University of Padova, Padova, Italy; [2]Istituto di Ricerca Pediatrica (IRP), Padova, Italy and [3]Pediatric Hematology-Oncology, University of Oklahoma Health Sciences Center, Oklahoma City, OK, USA. Correspondence: Dr M Pigazzi, Dipartimento della Salute della Donna e del Bambino–SDB, Clinica di Oncoematologia Pediatrica, Università degli Studi di Padova, Via Giustiniani 3, Padova 35128, Italy.
E-mail: martina.pigazzi@unipd.it
Received 23 December 2015; revised 7 March 2016; accepted 11 April 2016; accepted article preview online 27 April 2016; advance online publication, 24 May 2016

MATERIALS AND METHODS

Zebrafish maintenance and microinjection

Embryos were obtained from natural crosses, and 2 nl of solution was microinjected into the yolk of fertilized one-cell-stage embryos. Purified plasmids were diluted at a final concentration of 30 ng/μl, and transposase mRNA at a final concentration of 25 ng/μl in Danieau solution (58 mM NaCl, 0.7 mM KCl, 0.4 mM $MgSO_4$, 0.6 mM $Ca(NO_3)_2$, and 5 mM HEPES (pH 7.6)), with 10% phenol red. Embryos were reared in a 28.5 °C incubator with 12/12-hours dark/light cycle. Fluorescence was monitored on a Nikon SMZ1500 zoom stereomicroscope (Nikon Instruments Inc., Tokyo, Japan).

Flow cytometry

Whole adult zebrafish were killed with 2 mg/ml MS-222 at pH 7 (Tricaine; Sigma-Aldrich, St Louis, MO, USA). Kidney marrow and abdominal mass were isolated. Cells were homogenized in protease solution (Collagenase/Dispase 1:200, DNAse 1:1000, $MgCl_2$ 1:1000 in phosphate-buffered saline) at 37 °C for 30 min. The whole suspension was filtered through a 45 μm cell strainer, and then analyzed at BD FACS Aria III (Becton Dickinson, Milano, Italy) for cell size (FSC) and granularity (SSC). For differentiation experiments, cells were treated with ATRA (Sigma-Aldrich) at a final concentration of 5 μM. At 24, 48 and 72 h after treatment, the specific human cell marker CD11b-PE (Beckman Coulter, Brea, CA, USA) was detected by flow cytometry to determine myeloid differentiation.

Microarray data analysis

Total RNA was extracted from kidney marrow of 14-month-old CREB-zebrafish ($n = 5$) and control zebrafish ($n = 5$) and from bone marrow of 85 pediatric patients with *de novo* AML at diagnosis. RNA concentration was determined using QBit 2.0 Fluorometer (Life Technology, Carlsbad, CA, USA). RNA quality and purity control was assessed on the Agilent Bioanalyzed 2100 (Agilent Technologies, Santa Clara, CA, USA). The GeneChip Zebrafish Genome Array and the GeneChip Human Transcriptome Array 2.0 (Affymetrix, Santa Clara, CA, USA) were used for the microarray experiments. *In vitro* transcription, hybridization and biotin labeling were performed according to GeneChip 3'IVT Express kit protocol and GeneChip Hybridization, Wash, and Stain Kit (Affymetrix), respectively. Microarrays data (CEL files) were generated using Affymetrix GeneChip Command Console Software (AGCC). Microarray data (.CEL files) were analyzed using Command Expression Console (Affymetrix). Microarrays data have been deposited in NCBI Gene Expression Omnibus and are accessible through the GEO accession number GSE71270 for zebrafish (http://www.ncbi.nlm.nih.gov/geo/query/acc.cgi?token=yhepywwkhrorpif&acc=GSE71270) and GSE75461 for human AML (http://www.ncbi.nlm.nih.gov/geo/query/acc.cgi?token=mvslcaymfhyvtep&acc=GSE75461). The CEL files were normalized using the justRMA algorithm and analyzed for supervised and unsupervised analysis, using R-Bioconductor (Version 2.15.3, http://www.r-project.org/). Differentially expressed probe sets were identified by the Wilcoxon signed-rank test[32] and used to perform supervised analysis. The false discovery rate *q*-value of < 0.05 was considered significant for probe sets differently expressed between compared groups. Hierarchical clustering was used to group specimens in an unsupervised manner using Euclidean distance and Ward's method. Principal component analysis was performed using Partek Genomic Suite software (Partek Inc, http://www.partek.com) to integrate zebrafish signature with human genes. We converted the list of significantly differently expressed zebrafish genes into the human orthologs and subsequently we intersected them with the ChIP-Chip data of CREB binding in human tissues (http://natural.salk.edu/CREB/) to search for direct CREB targets. Moreover, we intersected them with the gene expression deposited data of the so-called Microarray Innovations in LEukemia (MILE) study program hematological diseases that included 898 human bone marrow samples of 542 AML, 76 chronic myeloid leukemia, 206 myelodysplastic syndrome and 74 healthy bone marrow.[33]

Gene set enrichment analysis

Gene Set Enrichment Analysis (GSEA) software version 4.0 was used to identify gene sets in the public domain that share the expression pattern found in the current study.[34] For each group of gene sets, GSEA calculates and evaluates the statistical significance of an enrichment score. The enrichment score reflects the degree to which a gene set is over-represented. We compared the gene expression signatures by collapsing the probe sets to gene vectors and using the signal-to-noise metric, the gene-set permutation type and 1000 permutations. As recommended by GSEA guidelines, only gene sets with a false discovery rate *q*-value of < 0.10 were considered. For help with interpreting the GSEA, go to http://www.broadinstitute.org/gsea/doc/GSEAUserGuideFrame.html%20Interpreting_GSEA_Results. The Nearest Template Prediction algorithm (NTP)[35] implemented as module of the Gene Pattern software (Broad Institute of Harvard and MIT, Boston, MA, USA) was used to predict the proximity of the expression pattern of molecular signatures deposited in the Molecular Signature Database (www.broadinstitute.org/gsea/msigdb) to each single patient's gene expression data using cosine distance. Only prediction with statistical significance ($P < 0.05$) were used for the heatmap generation.

Statistical methods

In patients and zebrafish cohort, probability of survival was estimated using the Kaplan–-Meier method and compared between groups through the log-rank test. Event-free survival was calculated from date of diagnosis to last follow-up or first event (failure to achieve remission, relapse, death, whichever occurs first) for patients, and from day of injection to first event (death or leukemic onset) for zebrafish. The Mantel–Byar test was used to calculate the cumulative incidence of relapse (CIR). Pearson's correlation test was used for RPPA data. Values are presented as mean ± s.d. Significance between experimental values was determined by Student's unpaired *t*-test, χ^2 test and Fisher's exact test. $^*P < 0.05$ was considered significant.

Study approval

All animal studies were approved by the animal care and use committee at the Health Ministry; 737/2015-PR approval.

See Supplementary Materials and methods for further details.

RESULTS

CREB overexpression perturbs primitive hematopoiesis and alters its target genes

To examine the role of CREB overexpression in hematopoiesis, we created a zebrafish model with exogenous CREB expression in the myeloid lineage under the control of a *pu.1* promoter:[36] we injected into one-cell-stage embryos a tol2 pDEST vector where enhanced green fluorescent protein (EGFP) was cloned in frame to the human *CREB* full length (indicated as CREB-zebrafish) and with a tol2 pDEST vector with EGFP to create the control group (indicated as controls; Supplementary Figure S1A). We monitored EGFP-positive cells during embryo development: at 24 h post fertilization (HPF), EGFP-positive cells were found in the anterior lateral mesoderm (Figure 1ai) and intermediate cell mass (Figure 1aii). Then, CREB activity as transcription factor through the cAMP response element (CREs) consensus regions binding was verified by reporter assays. We observed the coexpression of CREB together with a reporter plasmid containing 6× responsive CRE sequences upstream to the red fluorescent mCherry protein (Figure 1bi, controls, and Figure 1bii, CREB-zebrafish) in 90% of EGFP-CREB-expressing cells compared with 10% of EGFP-expressing cells in controls (Figure 1b; CREB, $n = 6$; controls (CTR), $n = 5$; $P < 0.001$). Moreover, we measured an increased luciferase activity in CREB-zebrafish compared with controls (mean CTR = 7.5 relative light unit (RLU), $n = 3$; mean CREB = 20.2 RLU, $n = 5$; $P < 0.05$, Supplementary Figure S1B). Once we verified the CREB activity, we monitored the effect of its exogenous expression during the primitive (20–24 HPF) and first wave of definitive hematopoiesis (30 HPF), as *pu.1* is expressed from 11 to 32 HPF.[37] Results showed that CREB-zebrafish had a significantly increased *gata1*-expressing cells in anterior lateral mesoderm and intermediate cell mass at 20 and 24 HPF and in posterior blood island at 30 HPF, as well as *mpo* in intermediate cell mass since 24 HPF (Figure 1c). We sought to understand whether CREB targets were also influenced during the first and the second wave of hematopoiesis by studying genes previously found upregulated in human bone marrow cells after CREB enforced expression.[1,3,8] At 24 HPF, CREB embryos showed an increase of *bcl2* expression in anterior lateral mesoderm, as well as

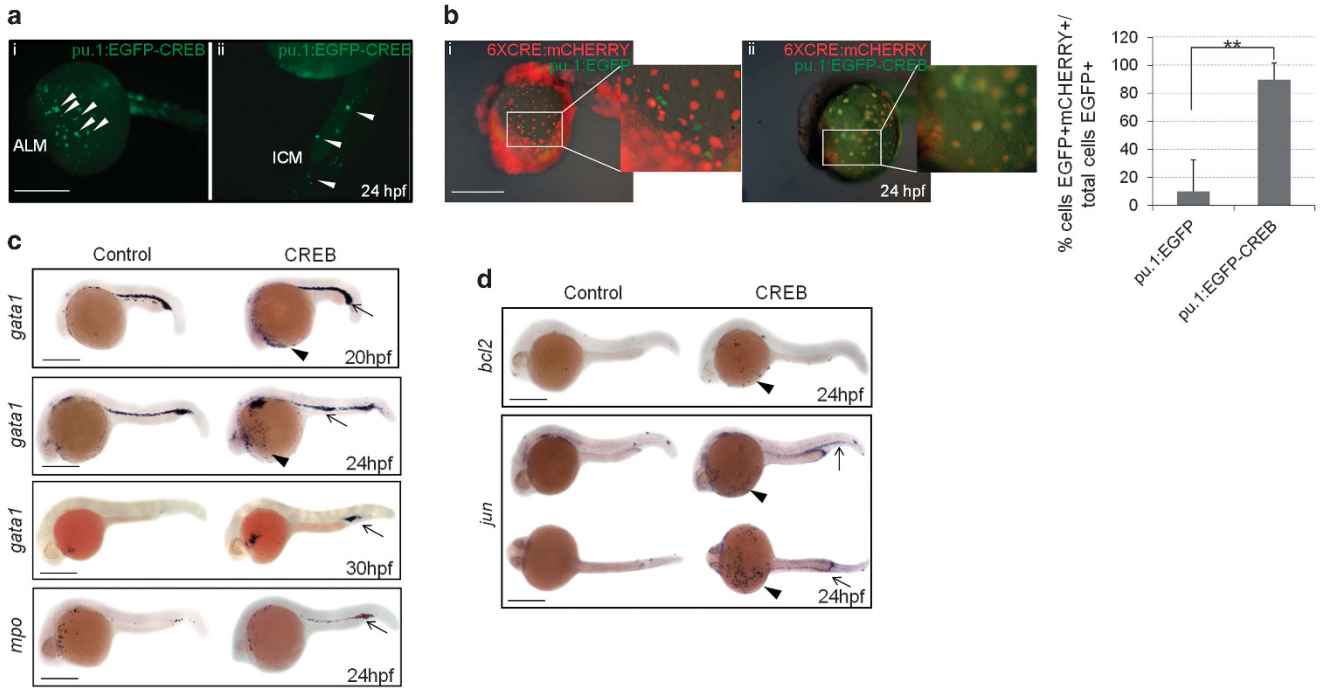

Figure 1. CREB works as a transcription factor and induces changes in hematopoietic markers and in CREB targets. (**a**) The EGFP expression in CREB-zebrafish embryos at 24 HPF is detected in (i) anterior lateral mesoderm (ALM), and in (ii) intermediate cell mass (ICM). (**b**) EGFP and mCHERRY expression in controls or CREB-zebrafish embryos coinjected with the 6xCRE:mCHERRY reporter plasmid (i and ii, respectively), showing overlapping signal in (ii). Histogram shows the percentage of EGFP-expressing cells that activate the 6XCRE:mCHERRY reporter in CREB-zebrafish (pu.1:EGFP-CREB) compared with controls (pu.1:EGFP) at 24 HPF (unpaired Student's *t*-test, $^{**}P < 0.001$). (**c**) Whole-mount *in situ* hybridization (WISH) showing increased *gata1* expression in the ALM (arrowheads) and ICM (arrows) at 20 and 24HPF, in the posterior blood island (PBI) at 30HPF and higher *mpo* expression in the ICM of CREB-zebrafish embryos compared with controls. (**d**) WISH showing the augmented expression of CREB target *bcl2* and *jun* at 24 HPF in ALM (arrowhead) and in ICM (arrows) of CREB embryos compared with controls. Scale bars: 500 μm.

a significant *jun* overexpression in both anterior lateral mesoderm and intermediate cell mass (Figure 1d). We also confirmed the upregulation of several CREB target genes by real-time quantitative PCR (data not shown).

CREB triggers leukemia in zebrafish

We followed the effects of CREB overexpression during CREB-zebrafish growth until adulthood: fish cohort comprised 98 CREB-zebrafish and 88 controls that were continuously observed to investigate the long-term effects of CREB forced expression. Between 9 and 14 months of age, CREB-zebrafish showed a sick phenotype characterized by a labored swimming with an evident abdominal mass (Figure 2a), and 77/98 (79%) were killed or found dead, whereas zebrafish controls grew healthy during the same period (2/88 were found dead without sick phenotype). We performed Kaplan–Meier survival analysis and found that event-free survival was significantly worse for CREB-zebrafish compared with controls (Figure 2b, $P < 0.001$, see also AML score at Supplementary Information). Cells from kidney marrow and tumor mass of CREB-zebrafish were dissociated and sorted: we observed the loss of hematopoietic precursors (P4: 17.4% in kidney of controls (Figure 2c) versus 2.7% in kidney (Figure 2d) and 0.5% in mass (Figure 2e) of AML CREB-zebrafish), an increased number of cells blocked at the myelomonocytic stage (P3: 38% in kidney of controls (Figure 2c) versus 43.4% in kidney (Figure 2d) and 51% in mass (Figure 2e) of AML CREB-zebrafish), an increased number of erythrocytes (P1: 20.1% in kidney of controls (Figure 2c) versus 49.6% in kidney (Figure 2d) and 46.4% in mass (Figure 2e) of AML CREB-zebrafish) and a strong impairment of the lymphocyte population (P2: 24.5% in kidney of controls (Figure 2c) versus 6% in kidney (Figure 2d) and 2.1% in mass (Figure 2e) of AML CREB-zebrafish). Moreover, 11/16 (69%) AML were morphologically defined as monocytic leukemia (French–American–British (FAB) M4–M5 by May Grunwald-Giemsa Figures 2f–h), 4/16 showed FAB M6 and one case was classified as M0. Then, sagittal tissue sections were subjected to histological analysis, revealing a large abdominal mass in CREB-zebrafish (Figures 3a and b, $n = 25$). Using higher magnification, we observed that in CREB-zebrafish the normal kidney structures were disrupted because of the infiltration of clonal cancer cells (Figures 3di and ii) compared with the kidney marrow of controls that was composed of tubules and glomeruli (Figures 3ci and ii). The same leukemic cells formed an abdominal mass (Figures 3ei and ii) and were also localized in extramedullary organs such as liver (Figures 3fi and ii) and heart (Figures 3gi and ii). The analysis of α-naphthyl acetate esterase activity confirmed the positivity of the monocytic leukemic cells (Figures 3hi and ii). Furthermore, we documented that the leukemic cells were CREB overexpressing (Figures 3i–k) and highly proliferating (Figures 3l–n). Infiltrating leukemic cells in the liver and heart were shown to have the same monocytic origin (Figures 3o–s).

Gene expression signature of CREB-induced AML resembles human AML

To identify the transcriptional activity induced by CREB overexpression, we performed gene expression analysis of kidney marrow from CREB-zebrafish and controls. CREB-zebrafish correctly clustered by using an unsupervised hierarchical cluster analysis (Figure 4a, dendrogram). Class comparison analysis identified a statistically significant signature of 258 genes differentially expressed (log2 false discovery rate *q*-value < 0.05) between CREB-zebrafish and controls (Figure 4a heatmap; Supplementary Table S1). Interestingly, inside this CREB-zebrafish signature we

identified 171 human homologous genes, of which 115 and 56 genes were respectively up- and down-regulated. To test the *bona fide* of this zebrafish AML model, we performed a principal component analysis using the list of human homologous genes that had >1.3-fold change of expression in the CREB signature to cluster the patients of the MILE study.[33] Of note, principal component analysis was able to distinguish AML patients from the rest of the hematological diseases (Figure 4b, red dots). Overall, these results support CREB-zebrafish as an appealing model for investigating CREB-mediated leukemogenesis at a transcriptome level. We recognized as CREB target 92 out of 171 (54%) human homologous differentially expressed genes (by using CREB target gene

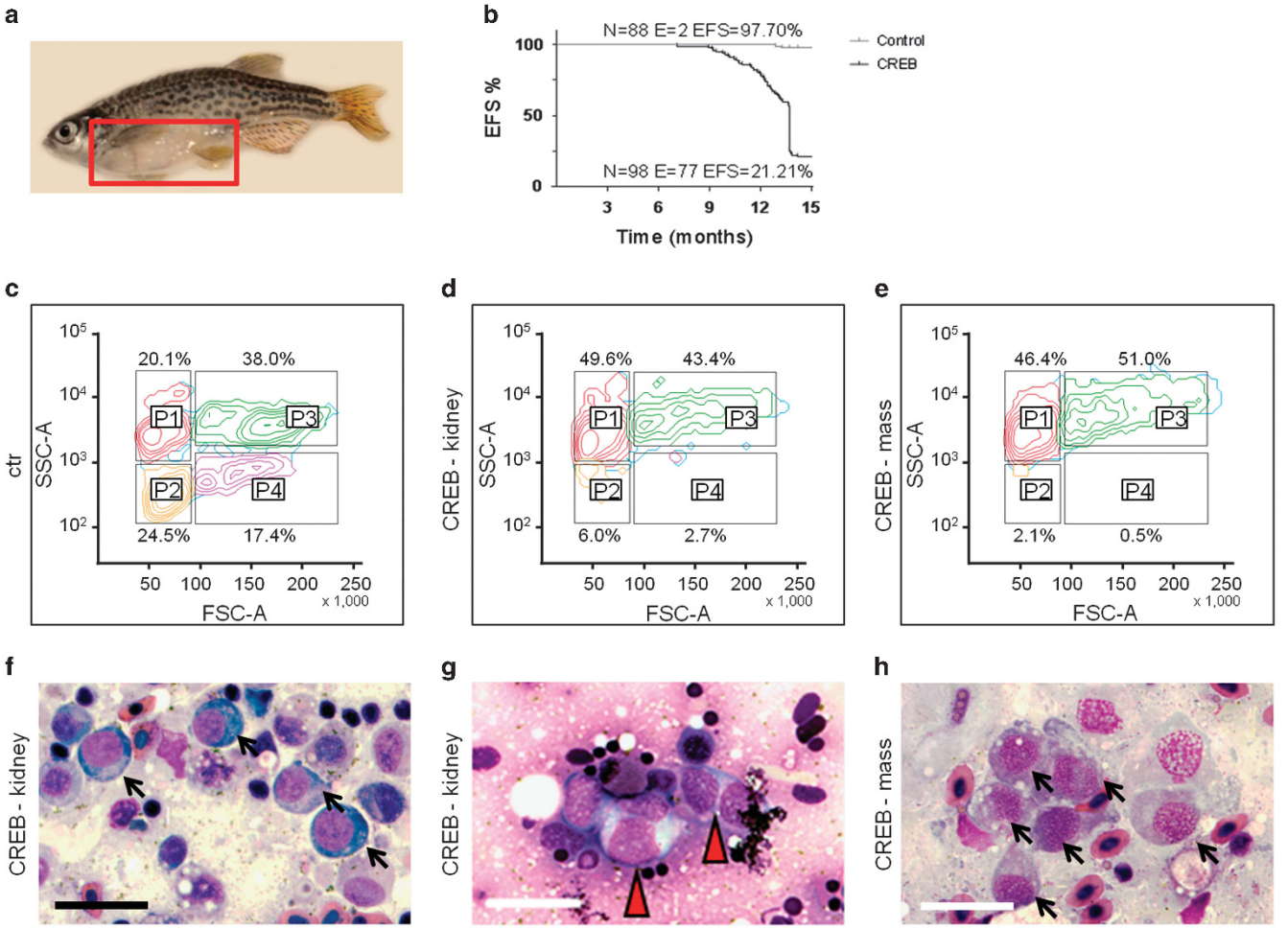

Figure 2. CREB triggers myeloid transformation. (**a**) Representative phenotype of leukemic CREB-zebrafish with abdominal mass (box). (**b**) Event-free survival (EFS) calculated for CREB-zebrafish compared with controls was statistically significant ($P < 0.001$). E, number of events; *n*, number of zebrafish. (**c–e**) Representative results of flow cytometric analysis from kidney of control (**c**) and CREB-zebrafish (**d**) and from abdominal mass of CREB-zebrafish (**e**) at the onset of leukemic phenotype. Gated populations are as follows: erythrocytes (P1), lymphocytes (P2), granulocytes and monocytes (P3) and blood cell precursor (P4). Population of cells are described as percentage of total cells. Cell size is represented by forward scatter (FSC), and granularity is represented by side scatter (SSC). (**f–h**) May Grunwald-Giemsa staining staining of kidney imprints. (**f**, **g**) Representative kidney cellular morphology of leukemic CREB-zebrafish, showing abnormal hematopoiesis characterized by the preponderance of monocytic cells (**f**, black arrows) and some binucleated monocytes (**g**, red arrowhead). Morphology of abdominal mass cells of leukemic CREB-zebrafish revealed monocytic cells (**h**, black arrows). Scale bars: 10 μm.

Figure 3. CREB-zebrafish develop myeloid leukemia with monocytic CREB-overexpressing blasts. Hematoxylin and eosin (H&E) histochemical staining of control and CREB-zebrafish (aged 13 months). (**a**, **b**) H&E staining of sagittal zebrafish sections (scale bar: 500 μm), demonstrating abdominal mass in AML CREB-zebrafish (red box). (**c–g**) High-power imaging of H&E staining: kidney tissue of control (**ci**, ii) and CREB-zebrafish (**di**, ii), showing disrupted kidney structures and presence of highly disorganized clonal infiltrated cells that display characteristic morphology of the myeloid lineage. Abdominal mass of CREB-zebrafish (**ei**, ii), displaying clonal cells with open chromatine texture, typical of cancer cells (arrows). Infiltration of cancer cells in liver (arrows in **fi**, ii) and in heart (arrows in **gi**, ii) of leukemic CREB-zebrafish. Acid α-naphthyl acetate esterase (ANAE) activity assay on imprints of control kidney (**hi**) and mass of diseased zebrafish (**hii**). (**i–k**) CREB immunohistochemical staining: kidney tissue from control zebrafish show some CREB-expressing cells (**li** and ii), whereas in CREB-zebrafish all leukemic cells in the kidney (**ji**, ii) and in the abdominal mass (**ki**, ii) are CREB expressing. (**l–n**) Proliferating cell nuclear antigen (PCNA) immunohistochemical staining: kidney tissue from control zebrafish show few PCNA-positive cells (**li**, ii). Leukemic cells of CREB-zebrafish in the kidney (**mi**, ii) and in the abdominal mass (**ni**, ii) display high number of PCNA-positive cells. (**o–s**) *In situ* hybridization of monocyte-specific *l-plastin* probe: weak signal is detected in kidney of controls (**o**), whereas strong signal is found in CREB-zebrafish kidney (**p**, arrows) and abdominal mass (**q**). In the liver and heart of CREB-zebrafish, positive signal is detected in the infiltrated myeloid cells (**r** and **s**, respectively, arrows). Scale bars: 50 μm.

database,[38] Supplementary Table S2). To identify the genes that could have an important role in mediating CREB-induced AML, we intersected them with the published data set of genes found to be differentially expressed in human pediatric AML versus healthy bone marrow,[9] finding 20 CREB target genes in common between zebrafish and the human AML (Figure 4c, Supplementary Table S3 and

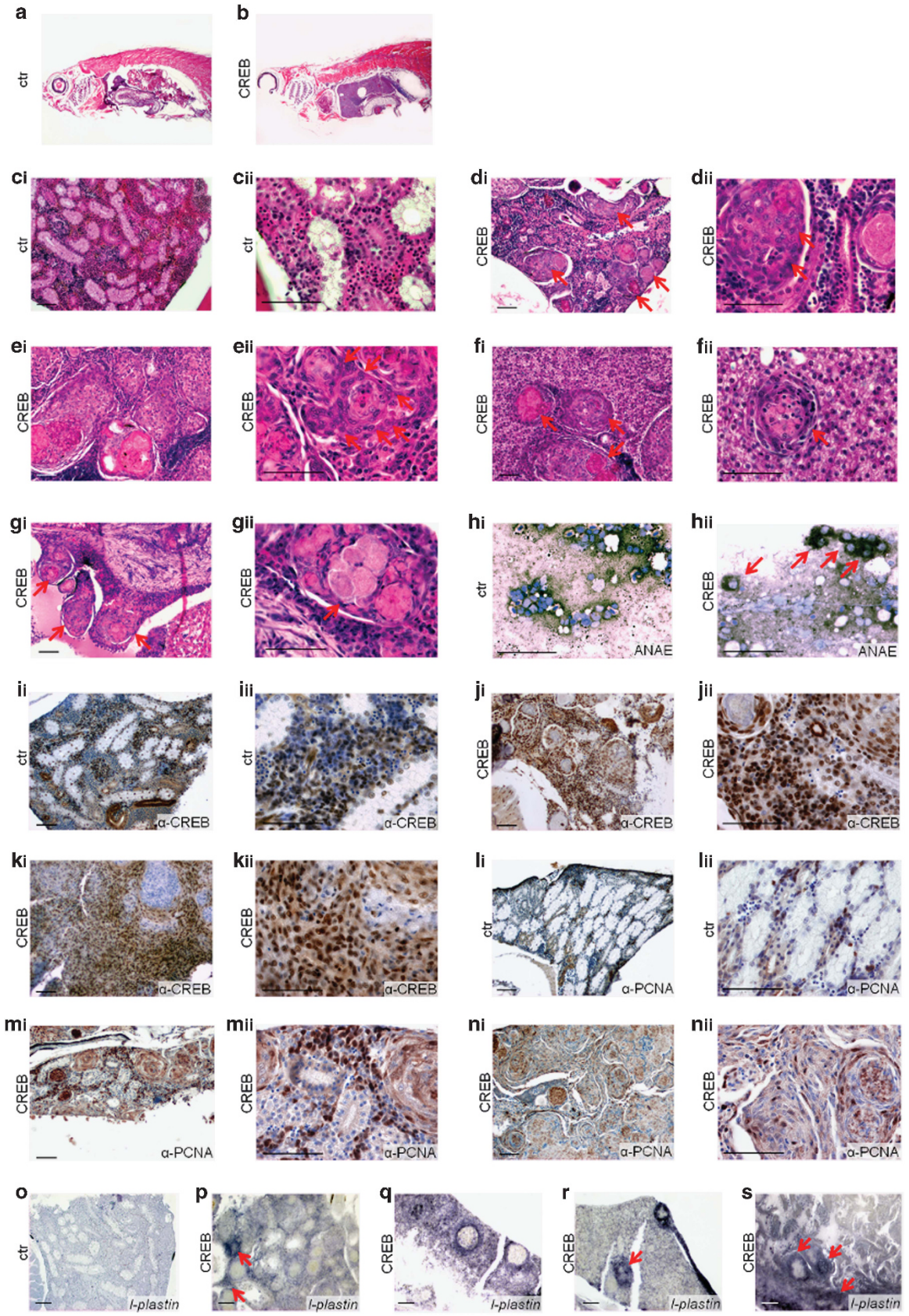

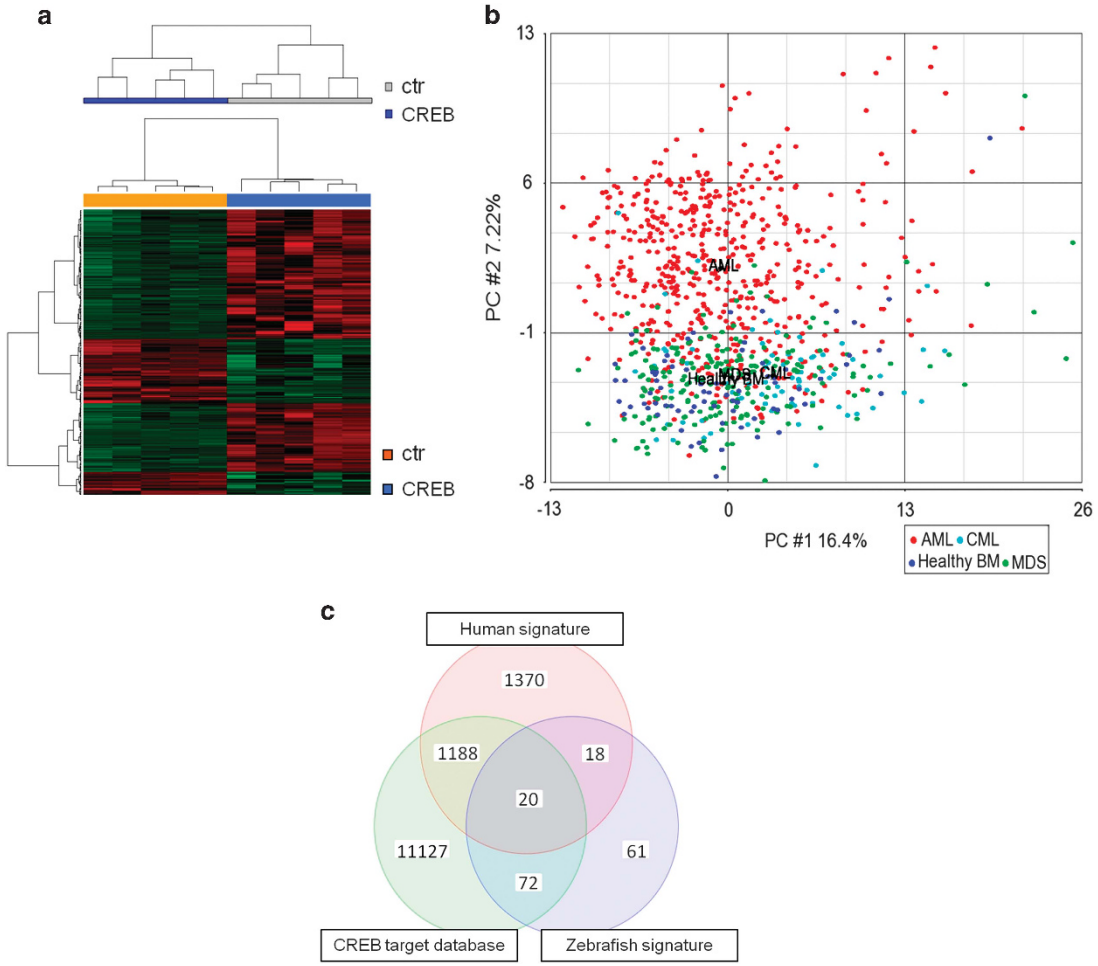

Figure 4. CREB-induced AML resembles childhood AML. (**a**) Unsupervised gene expression analysis of RNA extracted from kidney marrow of 5 samples of control zebrafish and 5 samples of CREB-zebrafish distinguishes the two groups (upper dendrogram). Class comparison analysis identified a statistically significant signature of 258 genes differentially expressed between CREB-zebrafish and controls (log2 false discovery rate (FDR) *q*-value < 0.05). (**b**) Principal component (PC) analysis using the 92 human homologous genes with a >1.3-fold change (FC) of expression identified by the CREB signature in the MILE cohort of 898 bone marrow samples (542 AML, 76 chronic myeloid leukemia (CML), 206 myelodysplastic syndrome (MDS) and 74 healthy bone marrow (BM))[33] reveals that zebrafish signature is able to cluster the AML samples (red) from the other hematological diseases. (**c**) Venn diagram showing the 20 common genes resulting from the intersection between the 171 human homologous genes differentially expressed in CREB-zebrafish, the human signature of AML samples versus healthy bone marrow[9] and the human CREB targets (from the ChIP-chip database[38]).

Supplementary Figure S2). We confirmed at proteomic levels the correlation of CREB activation[4] with a series of the 20 abovementioned genes in a cohort of 66 AML patients (Supplementary Table S4). Among these selected genes, we focused on *C/EBPδ*, as it belongs to the C/EBP family of transcription factors that regulate myeloid differentiation,[39–41] the main oncogenic process found deregulated in CREB-zebrafish. We evaluated C/ebpδ protein expression in zebrafish, documenting its higher expression in the kidney marrow of CREB-zebrafish (Supplementary Figure S3A), and in pediatric AML (Supplementary Figure S3B, $r = 0.79$). Subsequently, we studied the role of CREB as transcription factor over *C/EBPδ in vitro: CREB* silencing in AML primary cells decreased *C/EBPδ* expression in both mRNA and proteins (Supplementary Figures S4A and B), whereas *C/EBPδ* levels increased after overexpressing exogenous *CREB* in healthy bone marrow primary cells (Supplementary Figure S4C).

C/EBPδ expression define a new pediatric AML subgroup

C/EBPδ expression was evaluated in a cohort of pediatric AML ($n = 85$) dichotomized into groups including the upper quartile (Q1, $n = 22$) and the lower three quartiles (Q2–4, $n = 63$). It was revealed in patients for whom we had clinical data available ($n = 76$) that in the quartile with the highest *C/EBPδ* expression, those affected by a monocytic AML (classified by FAB[42] classes M4 and M5) were overrepresented (Q1 = 7/19, 37%) as compared with the other three quartiles (Q2–4 = 12/57, 21%). Then, we validated this association by using two publicly available Gene Expression Omnibus (GEO) databases: the MILE (48 pediatric AML patients, GEO: GSE13204)[33] and the St Jude (110 pediatric AML patients, GEO: GSE13204).[43] MILE cohort showed that FAB M4 and M5 AML were 11 out of 12 (92%) in Q1 versus 18 out of 36 (50%) in Q2–4 ($P < 0.05$); in St Jude cohort, FAB M4 and M5 AML were 22 out of 29 (76%) in Q1 versus 21 out of 81 (26%) in Q2–4 ($P < 0.0001$). Both studies corroborated the correlation between *C/EBPδ* over-expression and the block of myeloid differentiation at monocytic stage in pediatric AML. To investigate whether patients with both features may distinguish a novel AML subgroup we performed survival and gene enrichment analysis. Survival analysis suggested a trend toward lower event-free survival (Q1 = 40.1% versus Q2–4 = 50.86%, not significant), and a higher risk of relapse in Q1 group than in Q2–4 groups (CIR Q1 = 47.61% versus Q2–4 = 28.38%, not significant; Figure 5a). Interestingly, when we

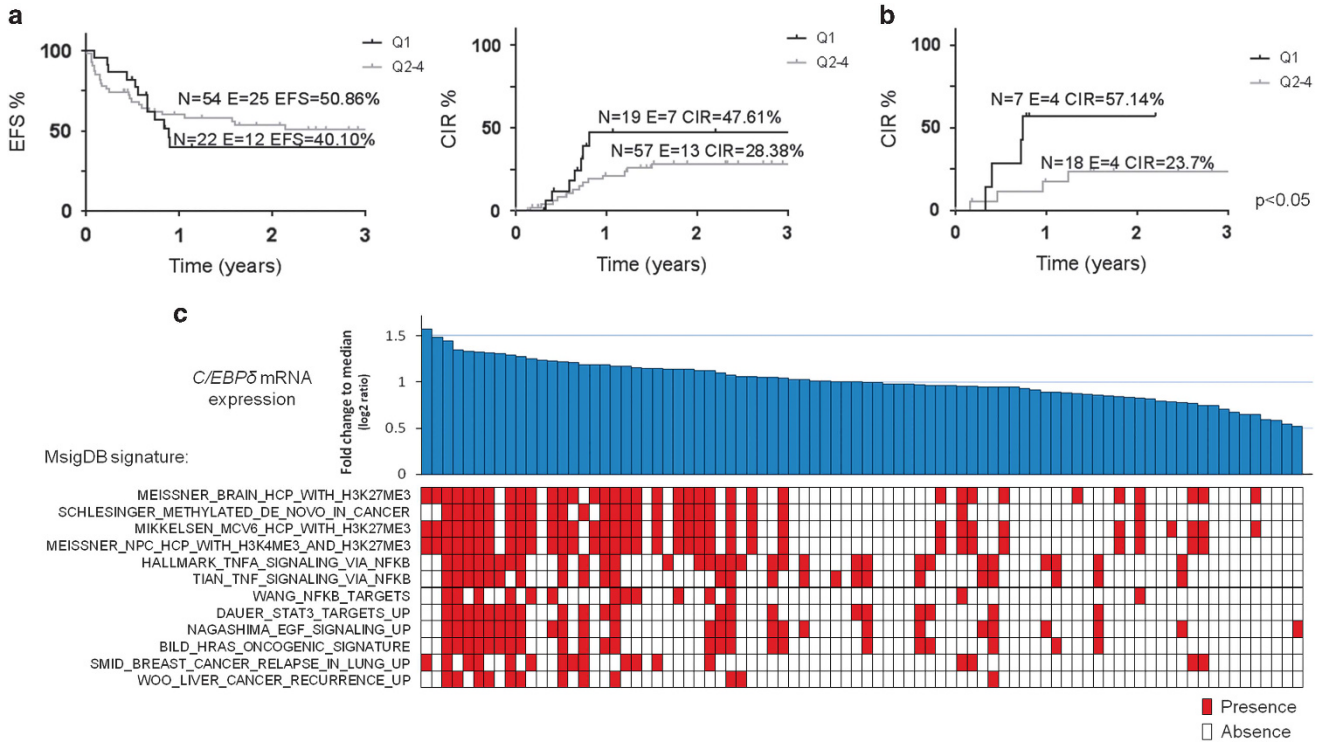

Figure 5. High C/EBPδ expression defines a subclass of high risk AML. (**a**) Event-free survival (EFS, left) and cumulative incidence of relapse (CIR, right) calculated for patients who express C/EBPδ at higher level (Q1) and lower level (Q2–4). (**b**) CIR calculated for patients who express different C/EBPδ levels (Q1 versus Q2–4), and FAB ⩾M4 was statistically significant ($P < 0.05$). E, number of events; *n*, number of patients. (**c**) The 85 pediatric AML were rank-ordered according to C/EBPδ expression. The presence of significant Molecular Signature DataBase (MSigDB) gene patterns identified by NTP algorithm are indicated by red boxes ($P < 0.05$). Statistical differences between groups Q1 ($n = 22$) and Q2–4 ($n = 63$) were assessed by Fisher's exact test, and all the gene signatures were statistically significant ($P < 0.05$).

considered the CIR among the patients with FAB ⩾M4, we revealed that they had a significantly higher risk of relapse if they overexpressed *C/EBPδ* (CIR Q1 = 57.1% versus Q2–4 = 23.7%, $P < 0.05$, Figure 5b). AML patients were then ranked by *C/EBPδ* expression and enrichment of molecular signatures was evaluated: by NTP[35] we identified the H3K27Me3 and H3K4Me3 as peculiar biological pathways characterizing high-C/EBPδ-expressing AML. Genes associated with nuclear factor-κB, HRAS pathways[44–50] and signatures of tumor recurrence were also concordantly and significantly enriched in Q1 patients (Figure 5c, $P < 0.05$; Supplementary Table S5). These novel biological features support the findings of a new subgroup of AML with biological and clinical specific features. GSEA confirmed an enrichment for several signatures related to M4–M5 FAB in Q1 (Supplementary Table S6).

CREB blocks myeloid differentiation through C/EBPδ overexpression

We conducted further experiments to investigate C/EBPδ role in myeloid differentiation. We took advantages of a previously created cell line[3] where CREB protein levels were reduced to physiological levels (here called HL60$^{(CREB-)}$) compared with the control cell line called HL60$^{(CREB+)}$ (Supplementary Figure S5A). We verified that *C/EBPδ* was lowered in HL60$^{(CREB-)}$ cell line compared with HL60$^{(CREB-)}$ (Supplementary Figure S5B). To investigate the role of CREB in myeloid differentiation program, we evaluated CD11b expression in the abovementioned cell lines after treatment with all-*trans* retinoic acid (ATRA). Results showed that HL60$^{(CREB-)}$ differentiated to a greater extent as compared with HL60$^{(CREB+)}$ after ATRA exposure: CD11b-positive cells were 16%, 38.7% and 42% in HL60$^{(CREB+)}$ compared with 23.6%, 64% and 68.7% in HL60$^{(CREB-)}$ at 24, 48 and 72 h, respectively (Figure 6a), confirmed by cell morphology examination (Supplementary Figure S5C), suggesting that CREB plays a crucial role in terminal differentiation capacity of myeloid cells. To investigate whether *C/EBPδ* is the main mediator in driving this phenomenon, we silenced *C/EBPδ* gene in HL60 cell line treated with ATRA. We confirmed gene silencing by real-time quantitative PCR (Supplementary Figure S5D); by flow cytometry analysis we found that CD11b-positive cells were increased after *C/EBPδ* silencing and ATRA treatment compared with small interfering RNA negative control (Figure 6b: 10.6% vs 6.3% at 24 h; 22.9% vs 12.4% at 48 h; 42.5% vs 23.8% at 72 h), demonstrating that *C/EBPδ* silencing phenocopied CREB behavior in promoting terminal myeloid differentiation. To verify the synergy of CREB-C/EBPδ axis, we performed a rescue experiment by silencing *CREB* and overexpressing C/EBPδ in HL60 (Supplementary Figures S6A and B). After 6 h of transfection, cells were also treated with ATRA. CD11b expression measured 48 and 72 h post treatment was increased after CREB silencing and then rescued after C/EBPδ overexpression, both at basal condition (Figure 6c: siRneg+EV = 2, siR*CREB*+EV = 3.2, siR*CREB*+C/EBPδ = 1.6 at 48 h; siRneg+EV = 1.6, siR*CREB*+EV = 3.9, siR*CREB*+C/EBPδ = 2.2 at 72 h) and after ATRA exposure (Figure 6c: siRneg+EV = 6.1, siR*CREB*+EV = 8.4, siR*CREB*+C/EBPδ = 6.1 at 48 h; siRneg+EV = 7.8, siR*CREB*+EV = 15.8, siR*CREB*+C/EBPδ = 9.8 at 72 h).

DISCUSSION

In this study, we considered the overexpression of the transcription factor CREB as a sole mutational event that was revealed as capable of inducing myeloid leukemia *in vivo*. CREB overexpression altered zebrafish primitive hematopoiesis through the upregulation of myeloid and erythroid genes, detectable in embryos at 24 to 30 HPF. This feature could be considered a specific aberrant phenotype that represents a marker of the first

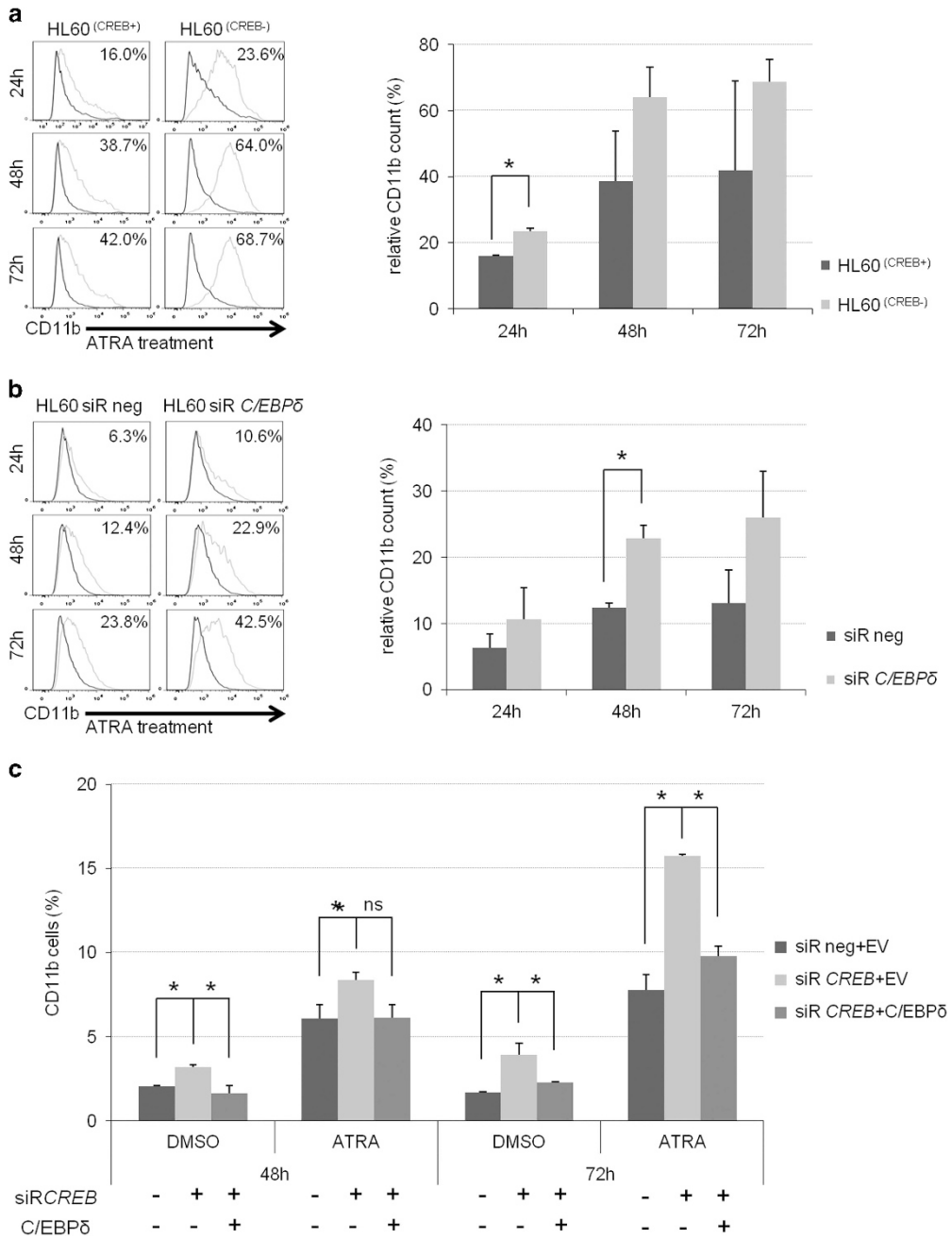

Figure 6. Lowered CREB levels induce myeloid differentiation, rescued by C/EBPδ overexpression. (**a**) ATRA treatment induced greater myeloid differentiation in HL60$^{(CREB-)}$ compared with HL60$^{(CREB+)}$ cell line at 24, 48 and 72 h. Expression of myeloid marker CD11b was analyzed by flow cytometry: a representative plot of the positive cells is showed on the left panel; histogram represents mean value of two independent experiments. The relative CD11b expression is normalized to the dimethyl sulfoxide (DMSO) treatment. Unpaired Student's *t*-test, $*P < 0.05$. (**b**) Silencing of *C/EBPδ* in HL60 cells enhanced ATRA-induced myeloid differentiation at 24, 48 and 72 h after treatment. Expression of myeloid marker CD11b was analyzed by flow cytometry: a representative plot of positive cells is showed on the left panel; histogram represents mean value of two independent experiments. The relative CD11b expression is normalized to the DMSO treatment. Unpaired Student's *t*-test, $*P < 0.05$. (**c**) Flow cytometry analysis of CD11b expression in HL60 after *CREB* silencing and C/EBPδ overexpression (EV, empty vector as plasmid control; siRneg, small interfering RNA (siRNA) negative control) after DMSO or ATRA treatment. Histogram represent mean value of three independent experiments. Unpaired Student's *t*-test, $*P < 0.05$.

CREB-induced oncogenic effects, providing the unique opportunity to develop high-throughput screening of small molecules and drugs in an *in vivo* myeloid leukemia model. In fact, adult CREB-zebrafish developed AML characterized by clonal mature monocytic blasts and severe loss of myeloid precursors, representing the first *in vivo* model of CREB-induced AML. To unravel the mechanism of leukemogenesis we investigated the biological mechanism enhanced by CREB to induce the block of myeloid differentiation, taking advantage of a human cell line previously modified to repress CREB levels and its downstream networks activation.[3] This cell line had a greater ability to differentiate upon ATRA treatment, conferring for the first time to CREB the ability to impair the myeloid terminal differentiation process *in vitro*, as largely observed in our CREB-zebrafish adult cohort. At this point, within the distinct functional groups of AML mutations,[51] CREB may be newly considered as a class II gene that affects the

myeloid differentiation process. Among the thousands of potential CREB target genes, to identify the main downstream player in triggering leukemia, we used gene expression profiles. We revealed that the CREB-induced leukemia in zebrafish resembled a human AML at transcriptome level and then, by integrating zebrafish-human and CREB databases, a new data set of 20 aberrantly expressed genes in common with pediatric AML have emerged.[9] Among the upregulated genes, the most intriguing was *c/ebpδ,* a member of the C/EBP family of transcription factors, among which C/EBPα has already been largely studied for its involvement in the regulation of myeloid differentiation.[39,40] Then, we validated the *C/EBPδ* expression in human AML by performing a screening in a large cohort of pediatric AML. *C/EBPδ* was found highly expressed particularly in the subgroup of patients affected by a monocytic leukemia (FAB M4–M5); this finding was also confirmed by two independent previously published pediatric AML cohorts[33,43] supporting CREB-zebrafish as a useful translational model. Furthermore, C/EBPδ highest levels were correlated with a new subgroup of AML patients with a significant higher risk of leukemia relapse. In order to characterize these AML, we interrogated gene expression enrichment analysis identifying nuclear factor-κB, HRAS and STAT3 oncogenic pathway activation. Interestingly, the molecular signaling of H3K27 trimethylation was particularly represented among these C/EBPδ-overexpressing patients, indicating that they may be influenced by aberrant gene repression. This latter finding suggests that further evaluation of demethylating agents may be tested in this zebrafish model as novel strategies for the FAB M4–M5 AML-overexpressing CREB and C/EBPδ.[44–46,48–50,52]

To definitively assign to C/EBPδ the key role in mediating CREB action, we documented that C/EBPδ phenocopied CREB effects by triggering the myeloid differentiation process arrest. Moreover, we demonstrated that increased C/EBPδ levels rescued the effects induced by CREB silencing, therefore acting downstream of CREB to block myeloid terminal differentiation.

Finally, this work presents an attractive *in vivo* model of CREB-mediated leukemogenesis that recapitulates a myeloid disease similar to a human AML with several biological and clinical relevances. The new axis CREB-C/EBPδ is here unraveled for the first time to contribute in CREB downstream network, and to delineate a new subtype of pediatric AML for whom novel therapeutic opportunities may be investigated within this zebrafish model.

CONFLICT OF INTEREST

The authors declare no conflict of interest.

ACKNOWLEDGEMENTS

We thank Dr Patrizia Porazzi for zebrafish manipulation, Dr Benedetta Accordi and Dr Valentina Serafin for RPPA analysis, Dr Chiara Frasson for cell sorting and Dr Luca Persano for tissue sectioning. This work was supported by grants from Cariparo, IRP-Istituto di Ricerca Pediatrica Città della Speranza Padova and Università degli Studi di Padova.

REFERENCES

1 Shankar DB, Cheng JC, Kinjo K, Federman N, Moore TB, Gill A *et al.* The role of CREB as a proto-oncogene in hematopoiesis and in acute myeloid leukemia. *Cancer Cell* 2005; **7**: 351–362.
2 Sandoval S, Pigazzi M, Sakamoto KM. CREB: a key regulator of normal and neoplastic hematopoiesis. *Adv Hematol* 2009; **2009**: 634292.
3 Pigazzi M, Manara E, Baron E, Basso G. ICER expression inhibits leukemia phenotype and controls tumor progression. *Leukemia* 2008; **22**: 2217–2225.
4 Sandoval S, Kraus C, Cho EC, Cho M, Bies J, Manara E *et al.* Sox4 cooperates with CREB in myeloid transformation. *Blood* 2012; **120**: 155–165.
5 Pigazzi M, Ricotti E, Germano G, Faggian D, Aricò M, Basso G. cAMP response element binding protein (CREB) overexpression CREB has been described as critical for leukemia progression. *Haematologica* 2007; **92**: 1435–1437.
6 Crans-Vargas HN, Landaw EM, Bhatia S, Sandusky G, Moore TB, Sakamoto KM. Expression of cyclic adenosine monophosphate response-element binding protein in acute leukemia. *Blood* 2002; **99**: 2617–2619.
7 Pigazzi M, Manara E, Beghin A, Baron E, Tregnago C, Basso G. ICER evokes Dusp1-p38 pathway enhancing chemotherapy sensitivity in myeloid leukemia. *Clin Cancer Res* 2011; **17**: 742–752.
8 Pigazzi M, Manara E, Baron E, Basso G. MiR-34b targets cyclic AMP-responsive element binding protein in acute myeloid leukemia. *Cancer Res* 2009; **69**: 2471–2478.
9 Pigazzi M, Manara E, Bresolin S, Tregnago C, Beghin A, Baron E *et al.* MicroRNA-34b promoter hypermethylation induces CREB overexpression and contributes to myeloid transformation. *Haematologica* 2013; **98**: 602–610.
10 Pui C-H, Carroll WL, Meshinchi S, Arceci RJ. Biology, risk stratification, and therapy of pediatric acute leukemias: an update. *J Clin Oncol* 2011; **29**: 551–565.
11 Pession A, Masetti R, Rizzari C, Putti MC, Casale F, Fagioli F *et al.* Results of the AIEOP AML 2002/01 multicenter prospective trial for the treatment of children with acute myeloid leukemia. *Blood* 2013; **122**: 170–178.
12 Gibson BES, Webb DKH, Howman AJ, De Graaf SSN, Harrison CJ, Wheatley K. Results of a randomized trial in children with Acute Myeloid Leukaemia: medical research council AML12 trial. *Br J Haematol* 2011; **155**: 366–376.
13 Abrahamsson J, Forestier E, Heldrup J, Jahnukainen K, Jónsson OG, Lausen B *et al.* Response-guided induction therapy in pediatric acute myeloid leukemia with excellent remission rate. *J Clin Oncol* 2011; **29**: 310–315.
14 Ribeiro RC. Advances in treatment of de-novo pediatric acute myeloid leukemia. *Curr Opin Oncol* 2014; **26**: 656–662.
15 Pigazzi M, Masetti R, Martinolli F, Manara E, Beghin A, Rondelli R *et al.* Presence of high-ERG expression is an independent unfavorable prognostic marker in MLL-rearranged childhood myeloid leukemia. *Blood* 2012; **119**: 1086–1087; author reply 1087–1088.
16 Manara E, Bisio V, Masetti R, Beqiri V, Rondelli R, Menna G *et al.* Core-binding factor acute myeloid leukemia in pediatric patients enrolled in the AIEOP AML 2002/01 trial: screening and prognostic impact of c-KIT mutations. *Leukemia* 2014; **28**: 1132–1134.
17 Balgobind BV, Raimondi SC, Harbott J, Zimmermann M, Alonzo TA, Auvrignon A *et al.* Novel prognostic subgroups in childhood 11q23/MLL-rearranged acute myeloid leukemia: results of an international retrospective study. *Blood* 2009; **114**: 2489–2496.
18 Vassal G, Zwaan CM, Ashley D, Le Deley MC, Hargrave D, Blanc P *et al.* New drugs for children and adolescents with cancer: the need for novel development pathways. *Lancet Oncol* 2013; **14**: e117–e124.
19 Bautista F, Di Giannatale A, Dias-Gastellier N, Fahd M, Valteau-Couanet D, Couanet D *et al.* Patients in pediatric phase I and early phase II clinical oncology trials at Gustave Roussy: a 13-year center experience. *J Pediatr Hematol Oncol* 2015; **37**: e102–e110.
20 Santoriello C, Zon LI. Hooked! Modeling human disease in zebrafish. *J Clin Invest* 2012; **122**: 2337–2343.
21 Jing L, Zon LI. Zebrafish as a model for normal and malignant hematopoiesis. *Dis Model Mech* 2011; **4**: 433–438.
22 Liu S, Leach SD. Zebrafish models for cancer. *Annu Rev Pathol* 2011; **6**: 71–93.
23 Davidson AJ, Zon LI. The 'definitive' (and 'primitive') guide to zebrafish hematopoiesis. *Oncogene* 2004; **23**: 7233–7246.
24 Langenau DM, Traver D, Ferrando Aa, Kutok JL, Aster JC, Kanki JP *et al.* Myc-induced T cell leukemia in transgenic zebrafish. *Science* 2003; **299**: 887–890.
25 Gutierrez A, Grebliunaite R, Feng H, Kozakewich E, Zhu S, Guo F *et al.* Pten mediates Myc oncogene dependence in a conditional zebrafish model of T cell acute lymphoblastic leukemia. *J Exp Med* 2011; **208**: 1595–1603.
26 Chen J, Jette C, Kanki JP, Aster JC, Look AT, Griffin JD. NOTCH1-induced T-cell leukemia in transgenic zebrafish. *Leukemia* 2007; **21**: 462–471.
27 Sabaawy HE, Azuma M, Embree LJ, Tsai H-J, Starost MF, Hickstein DD. TEL-AML1 transgenic zebrafish model of precursor B cell acute lymphoblastic leukemia. *Proc Natl Acad Sci USA* 2006; **103**: 15166–15171.
28 Zhuravleva J, Paggetti J, Martin L, Hammann A, Solary E, Bastie JN *et al.* MOZ/TIF2-induced acute myeloid leukaemia in transgenic fish. *Br J Haematol* 2008; **143**: 378–382.
29 Yeh JR, Munson KM, Elagib KE, Goldfarb AN, Sweetser DA, Peterson RT. Discovering chemical modifiers of oncogene-regulated hematopoietic differentiation. *Nat Chem Biol* 2009; **5**: 236–243.
30 Gutierrez A, Pan L, Groen RWJ, Baleydier F, Kentsis A, Marineau J *et al.* Phenothiazines induce PP2A-mediated apoptosis in T cell acute lymphoblastic leukemia. *J Clin Invest* 2014; **124**: 644–655.
31 Dworkin S, Heath JK, deJong-Curtain TA, Hogan BM, Lieschke GJ, Malaterre J *et al.* CREB activity modulates neural cell proliferation, midbrain-hindbrain organization and patterning in zebrafish. *Dev Biol* 2007; **307**: 127–141.
32 Wilcoxon F. Individual comparisons of grouped data by ranking methods. *J Econ Entomol* 1946; **39**: 269.

33 Haferlach T, Kohlmann A, Wieczorek L, Basso G, Te Kronnie G, Béné MC *et al.* Clinical utility of microarray-based gene expression profiling in the diagnosis and subclassification of leukemia: Report from the international microarray innovations in leukemia study group. *J Clin Oncol* 2010; **28**: 2529–2537.
34 Subramanian A, Kuehn H, Gould J, Tamayo P, Mesirov JP. GSEA-P: a desktop application for Gene Set Enrichment Analysis. *Bioinformatics* 2007; **23**: 3251–3253.
35 Hoshida Y. Nearest Template Prediction: a single-sample-based flexible class prediction with confidence assessment. *PLoS One* 2010; **5**: e15543.
36 Hsu K, Traver D, Kutok JL, Hagen A, Liu T-X, Paw BH *et al.* The pu.1 promoter drives myeloid gene expression in zebrafish. *Blood* 2004; **104**: 1291–1297.
37 Bertrand JY, Kim AD, Violette EP, Stachura DL, Cisson JL, Traver D. Definitive hematopoiesis initiates through a committed erythromyeloid progenitor in the zebrafish embryo. *Development* 2007; **134**: 4147–4156.
38 Zhang X, Odom DT, Koo S-H, Conkright MD, Canettieri G, Best J *et al.* Genome-wide analysis of cAMP-response element binding protein occupancy, phosphorylation, and target gene activation in human tissues. *Proc Natl Acad Sci USA* 2005; **102**: 4459–4464.
39 Alberich-Jordà M, Wouters B, Balastik M, Shapiro-Koss C, Zhang H, DiRuscio A *et al.* C/EBPγ deregulation results in differentiation arrest in acute myeloid leukemia. *J Clin Invest* 2012; **122**: 4490–4504.
40 Pabst T, Mueller BU, Zhang P, Radomska HS, Narravula S, Schnittger S *et al.* Dominant-negative mutations of CEBPA, encoding CCAAT/enhancer binding protein-alpha (C/EBPalpha), in acute myeloid leukemia. *Nat Genet* 2001; **27**: 263–270.
41 Hirai H, Yokota A, Tamura A, Sato A, Maekawa T. Non-steady-state hematopoiesis regulated by the C/EBPβ transcription factor. *Cancer Sci* 2015; **106**: 797–802.
42 Bennett JM, Catovsky D, Daniel MT, Flandrin G, Galton DA, Gralnick HR *et al.* Proposals for the classification of the acute leukaemias. French-American-British (FAB) co-operative group. *Br J Haematol* 1976; **33**: 451–458.
43 Radtke I, Mullighan CG, Ishii M, Su X, Cheng J, Ma J *et al.* Genomic analysis reveals few genetic alterations in pediatric acute myeloid leukemia. *Proc Natl Acad Sci USA* 2009; **106**: 12944–12949.
44 Meissner A, Mikkelsen TS, Gu H, Wernig M, Hanna J, Sivachenko A *et al.* Genome-scale DNA methylation maps of pluripotent and differentiated cells. *Nature* 2008; **454**: 766–770.
45 Schlesinger Y, Straussman R, Keshet I, Farkash S, Hecht M, Zimmerman J *et al.* Polycomb-mediated methylation on Lys27 of histone H3 pre-marks genes for de novo methylation in cancer. *Nat Genet* 2007; **39**: 232–236.
46 Mikkelsen TS, Hanna J, Zhang X, Ku M, Wernig M, Schorderet P *et al.* Dissecting direct reprogramming through integrative genomic analysis. *Nature* 2008; **454**: 49–55.
47 Liberzon A, Subramanian A, Pinchback R, Thorvaldsdóttir H, Tamayo P, Mesirov JP. Molecular signatures database (MSigDB) 3.0. *Bioinformatics* 2011; **27**: 1739–1740.
48 Tian B, Nowak DE, Jamaluddin M, Wang S, Brasier AR. Identification of direct genomic targets downstream of the nuclear factor-κB transcription factor mediating tumor necrosis factor signaling. *J Biol Chem* 2005; **280**: 17435–17448.
49 Wang H, Hertlein E, Bakkar N, Sun H, Acharyya S, Wang J *et al.* NF-kappaB regulation of YY1 inhibits skeletal myogenesis through transcriptional silencing of myofibrillar genes. *Mol Cell Biol* 2007; **27**: 4374–4387.
50 Bild AH, Yao G, Chang JT, Wang Q, Potti A, Chasse D *et al.* Oncogenic pathway signatures in human cancers as a guide to targeted therapies. *Nature* 2006; **439**: 353–357.
51 Gary Gilliland D, Griffin JD. The roles of FLT3 in hematopoiesis and leukemia. *Blood* 2002; **100**: 1532–1542.
52 Barski A, Cuddapah S, Cui K, Roh TY, Schones DE, Wang Z *et al.* High-resolution profiling of histone methylations in the human genome. *Cell* 2007; **129**: 823–837.

Supplementary Information accompanies this paper on the Leukemia website (http://www.nature.com/leu)